

East Tennessee State University

Digital Commons @ East Tennessee State University

ETSU Faculty Works

Faculty Works

8-11-2017

Limb Darkening and Planetary Transits: Testing Center-to-limb Intensity Variations and Limb-darkening Directly from Model Stellar Atmospheres

Hilding R. Neilson
University of Toronto

Joseph T. McNeil
East Tennessee State University

Richard Ignace
East Tennessee State University, ignace@etsu.edu

John B. Lester
University of Toronto Mississauga

Follow this and additional works at: <https://dc.etsu.edu/etsu-works>



Part of the [Stars](#), [Interstellar Medium](#) and the [Galaxy Commons](#)

Citation Information

Neilson, Hilding R.; McNeil, Joseph T.; Ignace, Richard; and Lester, John B.. 2017. Limb Darkening and Planetary Transits: Testing Center-to-limb Intensity Variations and Limb-darkening Directly from Model Stellar Atmospheres. *Astrophysical Journal*. Vol.845(1). 65. <https://doi.org/10.3847/1538-4357/aa7edf>
ISSN: 0004-637X

This Article is brought to you for free and open access by the Faculty Works at Digital Commons @ East Tennessee State University. It has been accepted for inclusion in ETSU Faculty Works by an authorized administrator of Digital Commons @ East Tennessee State University. For more information, please contact digilib@etsu.edu.



Limb Darkening and Planetary Transits: Testing Center-to-limb Intensity Variations and Limb-darkening Directly from Model Stellar Atmospheres

Copyright Statement

© 2017. The American Astronomical Society. All rights reserved.



Limb Darkening and Planetary Transits: Testing Center-to-limb Intensity Variations and Limb-darkening Directly from Model Stellar Atmospheres

Hilding R. Neilson¹ , Joseph T. McNeil^{2,3}, Richard Ignace² , and John B. Lester^{1,4}

¹ Department of Astronomy & Astrophysics, University of Toronto, 50 St. George Street, Toronto, ON M5S 3H4, Canada; neilson@astro.utoronto.ca

² Department of Physics & Astronomy, East Tennessee State University, Box 70652, Johnson City, TN 37614, USA

³ Department of Physics, University of Florida, P.O. Box 118440, Gainesville, FL 32611, USA

⁴ Department of Chemical & Physical Sciences, University of Toronto Mississauga, Mississauga, ON L5L 1C6, Canada

Received 2016 May 13; revised 2017 July 6; accepted 2017 July 7; published 2017 August 11

Abstract

The transit method, employed by *Microvariability and Oscillation of Stars (MOST)*, *Kepler*, and various ground-based surveys has enabled the characterization of extrasolar planets to unprecedented precision. These results are precise enough to begin to measure planet atmosphere composition, planetary oblateness, starspots, and other phenomena at the level of a few hundred parts per million. However, these results depend on our understanding of stellar limb darkening, that is, the intensity distribution across the stellar disk that is sequentially blocked as the planet transits. Typically, stellar limb darkening is assumed to be a simple parameterization with two coefficients that are derived from stellar atmosphere models or fit directly. In this work, we revisit this assumption and compute synthetic planetary-transit light curves directly from model stellar atmosphere center-to-limb intensity variations (CLIVs) using the plane-parallel ATLAS and spherically symmetric SATLAS codes. We compare these light curves to those constructed using best-fit limb-darkening parameterizations. We find that adopting parametric stellar limb-darkening laws leads to systematic differences from the more geometrically realistic model stellar atmosphere CLIV of about 50–100 ppm at the transit center and up to 300 ppm at ingress/egress. While these errors are small, they are systematic, and they appear to limit the precision necessary to measure secondary effects. Our results may also have a significant impact on transit spectra.

Key words: planets and satellites: fundamental parameters – stars: atmospheres

1. Introduction

The discovery of extrasolar planets in the past two decades has revolutionized our view of the universe and the prospects of discovering life around other stars. The rate of discovery has grown exponentially thanks to the transit detection method (Charbonneau et al. 2000) implemented through surveys such as the *Kepler* satellite (Borucki et al. 2010; Koch et al. 2010) and WASP (Pollacco et al. 2006). The results from these surveys are finding an assortment of planets ranging from super Earths to hot Jupiters, challenging the traditional picture of planet formation and evolution. However, to understand these transiting planets, it is also necessary to understand their host stars to achieve important constraints on the size of the planets and whether they have atmospheres.

Mandel & Agol (2002) developed an analytic method that is commonly employed for fitting transit light curves and that requires understanding the star’s radius and center-to-limb intensity variation (CLIV). As the planet passes in front of the star it blocks a small fraction of the star’s light, hence tracing a chord of the center-to-limb intensity variation. Typically, the intensity is represented by a simple limb-darkening law with either two or four free parameters (Claret 2000), similar to the analysis for understanding eclipsing binary light curves. However, because both stars in the eclipsing binary are bright, the light curves do not constrain the CLIV well (e.g., Popper 1984). Even though observations of eclipsing binary light curves have improved dramatically, the light curves are still fit using simple formulations for limb darkening (Prša & Zwitter 2005; Kirk et al. 2016). Similarly, microlensing observations provide even weaker constraints on limb-darkening laws (Dominik 2004; Fouqué et al. 2010). On the other

hand, interferometric observations are beginning to probe the details of stellar limb darkening, such as the impact of convection (Chiavassa et al. 2010) and the importance of extension in cool massive stars (e.g., Wittkowski et al. 2004, 2006a, 2006b).

Similarly, the precision of planetary-transit observations is now approaching the point where the details of the stellar atmosphere CLIV are becoming important for the analysis of the planet. To that end, Sing et al. (2009) and Sing (2010) developed a three-parameter limb-darkening law that is a significant improvement on the quadratic law, but provides no improvement to the Claret (2000) four-parameter law. Furthermore, Espinoza & Jordán (2015, 2016) carefully analyzed the biases induced by assuming various limb-darkening laws and found that the three-parameter law along with other square-root and logarithmic limb-darkening laws can provide more accurate measurements of transit properties than more commonly used linear and quadratic limb-darkening laws.

In turn, the transit light curves can also be used to test model stellar atmospheres. For example, Knutson et al. (2007) fit multi-wavelength observations of HD 209458 to measure limb-darkening coefficients (LDCs) that were compared with synthetic LDCs computed using the ATLAS stellar atmosphere code (Kurucz 1979). However, theory and observations disagreed. Claret (2009) also analyzed the observations of HD 209458 using LDCs computed with model stellar atmospheres that included different turbulent velocities, different procedures to compute the LDCs, and even different atmosphere codes, but disagreements between the predicted and observed light curves remained. This suggests a tension between theory and observations that needs to be resolved.

HD 209458 is not the only system challenging our understanding of limb darkening and stellar atmospheres. For instance, disagreements have been found to exist between theory and observations for the systems XO-1b, HAT-P-1b (Winn et al. 2007), HAT-P-11b (Deming et al. 2011), Kepler-5b (Kipping & Bakos 2011a, 2011b), CoRot-13b (Cabrera et al. 2010), and others. These disagreements, while not greatly affecting the measurements of the planetary properties, do raise questions about model stellar atmospheres and the precision of the light curve fits.

Howarth (2011) found that, at least for some cases, the disagreements can be resolved by accounting for the inclination of the system, defined by the impact parameter, b , the minimum distance between the center of the stellar disk and the transiting planet's path normalized to the star's radius:

$$b \equiv \frac{a \cos i}{R_*}, \quad (1)$$

where a is the planet's orbital semimajor axis and i is the orbital inclination. For a planet with an orbit inclined to our line of sight, the transit path is only a limited chord across the stellar disk, not the full diameter. Therefore, the LDCs must be altered accordingly, especially if there are errors in fitting the CLIV. Similar results were found by Müller et al. (2013).

While the results of Howarth (2011) and Müller et al. (2013) proved promising, they did not resolve the differences for all systems, and other factors have been considered. For example, starspots will change the stellar flux and the apparent effective temperature, meaning the theoretical LDCs will be computed from the wrong stellar atmosphere model (Csizmadia et al. 2013). Another factor is the method for fitting the LDCs. Kipping (2013) showed that observational fits are more sensitive to a linear combination of the LDCs that makes them more linearly dependent. A third factor is the role of the geometry of the stellar atmosphere on the star's CLIV; spherically symmetric model atmospheres produce different LDCs than the more commonly used plane-parallel model stellar atmospheres (Neilson & Lester 2011, 2012, 2013a, 2013b). However, none of these solutions have been shown to resolve all the differences.

In this work, we compare planetary-transit light curves computed using limb-darkening laws with those calculated directly from the model stellar atmosphere CLIV. We start in Section 2 by outlining the analytic approach for planet transits (Mandel & Agol 2002) to better understand the role of limb darkening. In Section 3, we describe the model atmosphere code and models chosen for this work as well as how the model LDCs are computed. In Section 4, we present results of the comparison between light curves computed using model CLIV and corresponding LDCs from a traditional two-parameter quadratic limb-darkening law. We compare the CLIV predictions with light curves computed assuming a more complex four-parameter limb-darkening law in Section 5. In Section 6, we extend the analysis to consider the sensitivity of limb darkening with respect to the impact parameter, i.e., different orbital inclinations, and in Section 7, we model the differences as a function of wavelength for transit spectroscopy. We summarize our work in Section 8.

2. Method

We compute planetary-transit light curves using either model stellar atmosphere CLIV or limb-darkening laws. We use model

stellar atmosphere CLIV from Neilson & Lester (2013b), computed using versions of the ATLAS9 stellar atmospheres code (Kurucz 1979) that assumes either plane-parallel or spherically symmetric geometry (Lester & Neilson 2008). The intensity profiles are computed for 1000 equally spaced values of μ , where $\mu \equiv \cos \theta$ and θ is the angle formed between a line-of-sight point on the stellar disk and the center of the stellar disk. The spacing of the μ points represent a significantly higher resolution than previous models (e.g., Wade & Rucinski 1985; Claret 2000). The intensity profiles are computed for the B , V , R , I , H , K , $CoRot$, and $Kepler$ wavebands and also include best-fit LDCs for a number of parameterized limb-darkening laws (Claret 2000; Claret et al. 2012).

The calculation of the planetary-transit light curves was done using the small-planet approximation of Mandel & Agol (2002). This approximation assumes that the portion of the star's surface being blocked by the transiting planet has a uniform brightness. Following Mandel & Agol (2002), this approximation is assumed to apply when $R_p \lesssim 0.1R_*$ and is parameterized as

$$\rho \equiv \frac{R_p}{R_*} \lesssim 0.1, \quad (2)$$

where R_p is the radius of the planet and R_* is the star's radius. This ratio corresponds approximately to Jupiter transiting the Sun or to a Uranus-size planet transiting a K dwarf star. While this is an approximation adopted to simplify the calculation of the light curve, we will show that the differences between our light curves scale approximately as $(R_p/R_*)^2$ and that errors introduced by assuming the small-planet approximation largely cancel out. For this assumption Mandel & Agol (2002) derived expressions for the star's relative flux, f , defined as

$$f \equiv \frac{\text{flux during transit}}{\text{unobscured flux}}. \quad (3)$$

There are three possible cases depending the projected separation between the center of the planet and the center of the star normalized by the stellar radius, represented as z , and the relative sizes of the planet and star given by ρ defined above. If the planet does not transit the star, the parameter $z > 1 + \rho$, which clearly gives $f(z) = 1$. If the planet grazes the stellar disk, $1 - \rho < z \leq 1 + \rho$, then

$$f(z) = 1 - \frac{I^*(z)}{4\Omega} \left[\rho^2 \cos^{-1} \left(\frac{z-1}{\rho} \right) - (z-1) \sqrt{\rho^2 - (z-1)^2} \right], \quad (4)$$

where

$$I^*(z) = (1-a)^{-1} \int_{z-\rho}^1 2rI(r)dr, \quad (5)$$

a is the planet's orbital semimajor axis, $r \equiv \sin \theta = \sqrt{1 - \mu^2}$, and the term Ω is determined by the limb-darkening law assumed. Using a Claret (2000) four-parameter (4-p) law,

$$\frac{I(\mu)}{I(\mu=1)} = 1 - \sum_{n=1}^4 c_n (1 - \mu^{n/2}) \quad (6)$$

gives

$$\Omega = \sum_{n=0}^4 c_n (n+4)^{-1}, \quad (7)$$

where $c_0 \equiv 1 - c_1 - c_2 - c_3 - c_4$. The third case is for the interior light curve, $z < 1 - \rho$,

$$f = 1 - \frac{\rho^2 I^*(z)}{4\Omega}, \quad (8)$$

where in this case

$$I^*(z) = (4z\rho)^{-1} \int_{z-\rho}^{z+\rho} 2rI(r)dr. \quad (9)$$

The star's intensity distribution contributes to the terms $I^*(z)$ and Ω through Equations (5), (7), and (9). The term Ω was defined by Mandel & Agol (2002) based on the four-parameter limb-darkening law, but more generally Ω is a flux-like variable such that $4\Omega = \int_0^1 2rI(r)dr$. In the following sections, we compute synthetic planetary-transit light curves using these definitions of 4Ω and $I^*(z)$.

3. Center-to-limb Intensity Variations and Limb-darkening Laws

To illustrate the quality of the fits provided by limb-darkening laws, we use a model stellar atmosphere with the effective temperature $T_{\text{eff}} = 5600$ K, gravity $\log g = 4.5$, and mass $M_* = 1.1 M_\odot$ from the grid of model stellar atmospheres computed by Neilson & Lester (2013b). That model assumes solar composition from the Kurucz (2005) opacity files and is computed for both plane-parallel and spherical symmetries. The plane-parallel geometry assumes that the depth of the atmosphere is small relative to the radius of the star, which simplifies the model radiative transfer greatly as the radiation field depends on depth only (Mihalas 1978). In that case, limb darkening is computed simply as an exponential scaling of the central radiation field. In spherical symmetry, one relaxes that assumption for a more physically realistic scenario where radiative transfer must be treated as a function of both depth and angle. As such limb darkening cannot be scaled relative to the central radiation field and must be calculated self-consistently, leading to a different structure as a function of angle, especially near the edge of the star.

The CLIV for each geometry is plotted in Figure 1 along with a best-fitting quadratic limb-darkening law of the form

$$\frac{I(\mu)}{I(\mu=1)} = 1 - u_1(1 - \mu) - u_2(1 - \mu)^2, \quad (10)$$

for the *B*, *V*, *R*, *I*, *H*, *K*, *CoRot*, and *Kepler* wavebands. This limb-darkening law clearly provides a better fit for the plane-parallel model CLIV than for the spherically symmetric model, but even for the plane-parallel models there is significant divergence near the limb of the star as $\mu \rightarrow 0$. The limb-darkening law deviates more significantly from the model CLIV for the spherically symmetric model. In terms of wavelength, the difference is greatest toward the near-infrared *H* and *K* bands, where the quadratic law fails to fit the sharp drop in intensity for the spherically symmetric models. The reason the CLIV has such a sharp drop and step-like structure is related to the total optical

depth in the photosphere at infrared wavelengths. At these longer wavelengths, the H^- opacity that dominates the absorption of radiation is smallest, and the photosphere is most transparent. Going from the center of the disk toward the limb the radiation comes from depths of the atmosphere where the temperature declines by only a small amount with increasing height, which leads to a relatively flat CLIV. However, when $\mu \leq 0.1$, which corresponds to $R \geq 0.99 R_*$, the atmospheric density becomes so small that the intensity drops rapidly. This indicates that the assumed limb-darkening law introduces errors for fitting light curves, particularly at these near-IR wavelengths.

In Figure 2, we repeat the comparison assuming the Claret (2000) 4-p limb-darkening law. The fits of the 4-p law are indistinguishable from the CLIV for the plane-parallel model. However, the best-fit four-parameter laws still do not fit the limb of the spherically symmetric model CLIV, especially the near-infrared *H* and *K* bands. Because the spherically symmetric model stellar atmospheres are more physically representative of actual stellar atmospheres, even the 4-p limb-darkening law will have deficiencies fitting planetary-transit light curves as observations achieve higher precision.

4. Comparison between CLIV and Quadratic Limb-darkening Laws

The next step is to compare how model CLIV and quadratic limb-darkening laws predict planetary-transit light curves using the analytic prescription of Mandel & Agol (2002). Their derivation is defined for an edge-on transit, i.e., an inclination $i = 90^\circ$ and an impact parameter $b = \cos i = 0$. That derivation also assumes the orbit of the transiting planet is circular. Light curves were calculated as a function of waveband, and we present the transit of the orbit in Figure 3 for the case of a plane-parallel model stellar atmosphere and corresponding limb-darkening coefficients.

The results shown in Figure 3 suggest that for plane-parallel models there is little difference between using a model CLIV or a limb-darkening law with best-fit coefficients. However, these plots are somewhat misleading because the plots are dominated by the transit depth, which is controlled by the central part of the stellar disk where the two representations agree. To distinguish between the two representations, we plot in Figure 4 the difference between the light curve derived from the computed CLIV, f_{CLIV} , and the light curve derived using the limb-darkening law, f_{LDL} , normalized by the transit depth. Because, by definition, $f \rightarrow 1$ at the stellar limb, the difference will go to zero at the ingress and egress of the planet's transit.

The difference between the CLIV and the limb-darkening coefficient-derived transits is most important when the planet goes through ingress/egress where the difference is more than about 100 ppm. This difference is not large, but it is significant and occurs at all wavelengths considered here. It further suggests that the difference is due solely to the inability of the quadratic limb-darkening law to fit the model CLIV, even for plane-parallel atmospheres. At $z = 0.9$, the difference in the *Kepler* transit flux is about 100 ppm, which is similar to the precision required to measure planetary oblateness (Seager & Hui 2002; Zhu et al. 2014). While the analysis is qualitative, this difference suggests that the predictions of Zhu et al. (2014) could be entangled with errors in the assumed limb-darkening law instead of planetary oblateness. While we cannot confirm

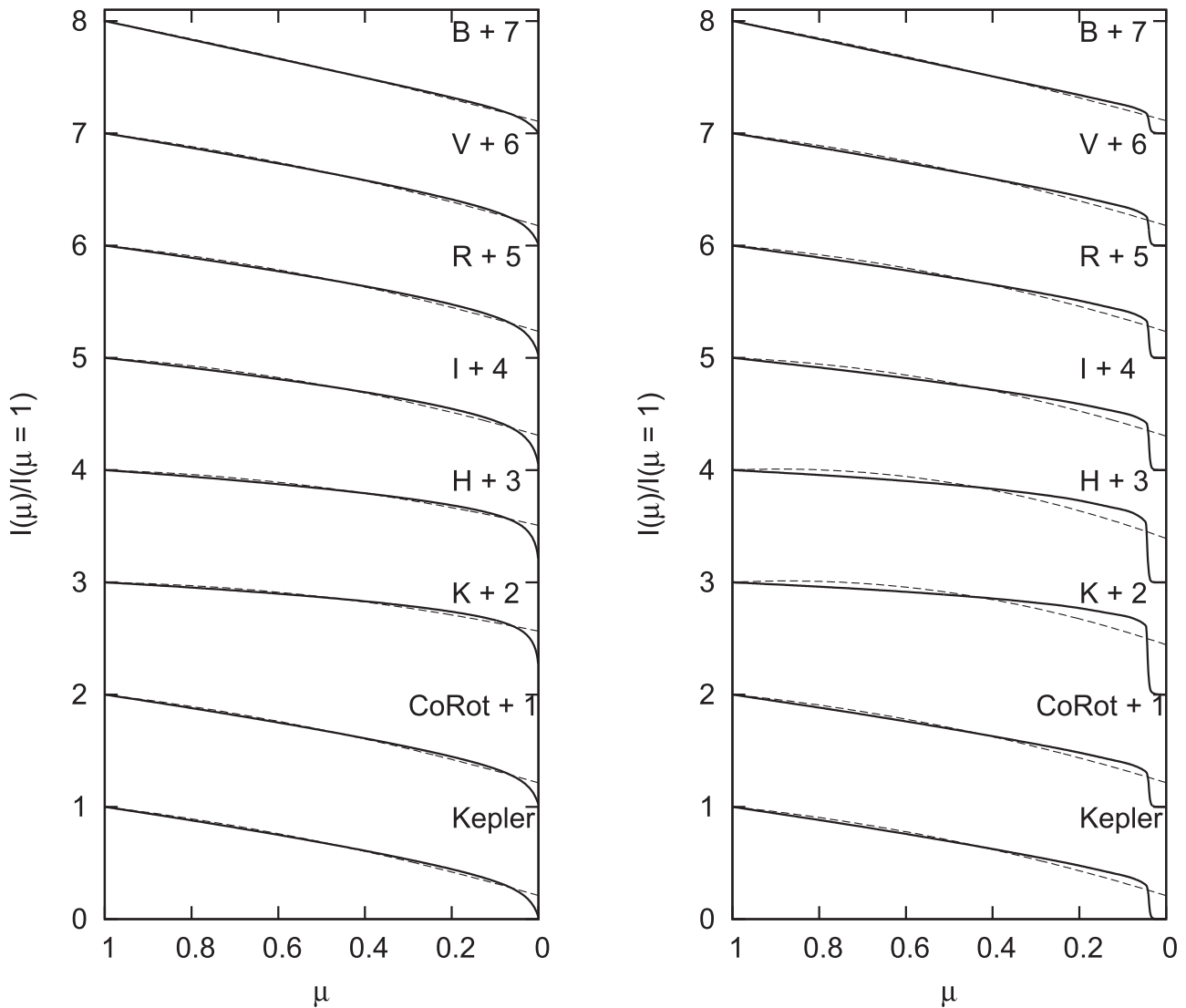


Figure 1. Comparison of wavelength-dependent model stellar atmosphere CLIV (solid line) with the corresponding best-fit quadratic limb-darkening law (dashed line) as a function of $\mu \equiv \cos \theta$, where, for clarity, each waveband’s profile is offset by the number next to the band’s name. (Left) Plane-parallel model atmosphere with $T_{\text{eff}} = 5600$ K and $\log g = 4.5$. (Right) Spherically symmetric geometry with luminosity $L = 0.8 L_{\odot}$, radius $R = 1.0 R_{\odot}$, and mass $M = 1.1 M_{\odot}$.

this suggestion, it is jarring that the differences between the light curves for a spherical and an oblate planet (Zhu et al. 2014, their Figure 1) have a similar behavior and magnitude to the differences between plane-parallel light curves using the CLIV and assuming a quadratic limb-darkening law in Figure 4.

We consider how this difference systematically affects the measurement of planetary radii relative to the stellar radii by computing the average difference between the CLIV and limb-darkening law versions of the planetary-transit light curves. This difference is not a measure of the error of the flux introduced by assuming a limb-darkening law. Instead, the difference provides a rough estimate of how much the surface area of the planet must change for the light curve computed with the limb-darkening law to agree most closely with the light curve computed using the CLIV. Because this average difference is a measure of the error of the relative surface area of the planet, it tells us about the various errors in transit spectroscopy (which is a differential measure of the surface area as a function of wavelength) and the uncertainty of the planetary radius. For all wavebands, the average difference between the light curve fluxes, hence the relative surface area

$(R_p/R_*)^2$, is about 50 ppm, suggesting an insignificant effect on the best-fit planet radius when we assume plane-parallel model stellar atmospheres.

This first test was for plane-parallel model stellar atmospheres, which have been the conventional approximation for the geometry of a star. However, a spherically symmetric geometry is a more geometrically realistic representation of a stellar atmosphere, especially for modeling CLIV (Neilson & Lester 2013a, 2013b). We repeat our analysis using a spherically symmetric model atmosphere and plot the difference between the planetary-transit light curves computed from the CLIV and its best-fit limb-darkening law in Figure 5. The differences are about $3\times$ greater than in Figure 4, reaching about 400 ppm. Because differences of this magnitude are now being detected in *Kepler* observations, it is necessary to fit the observations directly with the CLIV, or at least replace the traditional quadratic limb-darkening law with a more advanced representation.

Furthermore, for the plane-parallel model the difference at the transit center between using the CLIV and the best-fit limb-darkening coefficients varies by about 75 ppm at all wavebands. For the more geometrically realistic, spherically symmetric

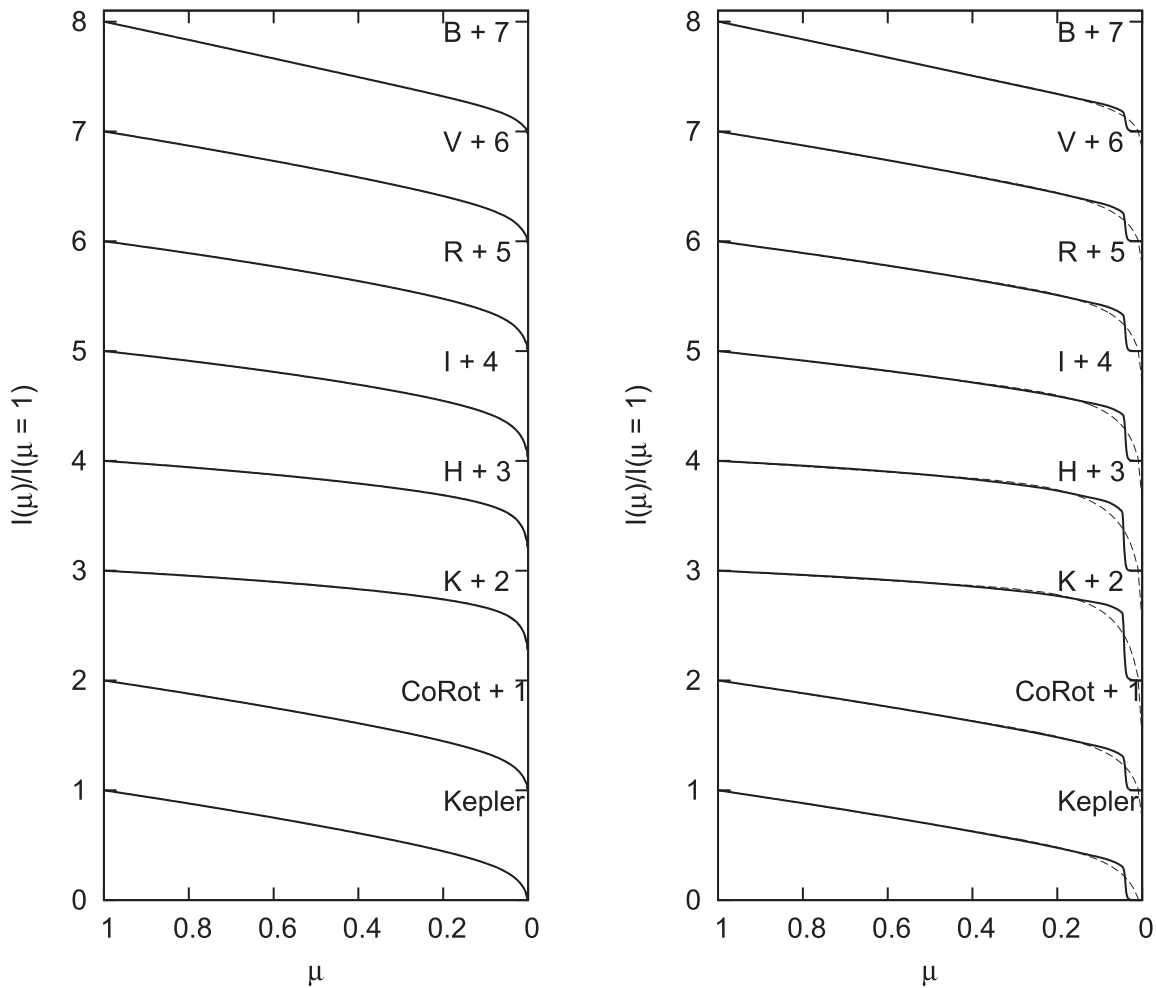


Figure 2. Comparison of wavelength-dependent model stellar atmosphere CLIV (solid line) with corresponding best-fit Claret (2000) four-parameter limb-darkening law (dashed line) as a function of $\mu \equiv \cos \theta$, where the model atmosphere assumes plane-parallel (left) and spherically symmetric geometry (right). The best-fit limb-darkening laws are indistinguishable from the plane-parallel CLIV in the left panel.

models those errors are greater, with the differences in transit depths varying from about 100 ppm at the shortest wavebands to about 200 ppm for *H* and *K* bands and about 150 ppm for the *CoRot* and *Kepler* wavebands. This error is smaller at transit center because, by definition, differences between the CLIV and limb-darkening laws decrease toward the center of the stellar disk. The differences are due solely to the failure for the limb-darkening law to conserve stellar flux.

For the spherical models the average difference between the CLIV and the limb-darkening law planetary-transit light curves is greater than that computed using plane-parallel models. At optical wavebands, the average difference is about 60–70 ppm, increasing in the near-IR up to 180 ppm. This suggests that some of the differences across the transit cancel allowing for a smaller error for measuring the relative planet radius. For the properties assumed here, the use of limb-darkening laws versus CLIV does not seem to cause large systematic uncertainties. However, there may be challenges for measuring transit spectroscopy, as the differences are a function of wavelength and may inhibit precise measurements of planetary atmospheres and composition.

The issue of conserving stellar flux from the model stellar atmosphere and the best-fit limb-darkening law is degenerate with the presence of unocculted starspots. Starspots affect transit light curves by decreasing the stellar flux and making the planet radius seem larger (e.g., Hellier et al. 2014; McCullough

et al. 2014). Because the spots are cooler than the star and follow a blackbody function, the spots have a differential effect on the stellar flux. As demonstrated in Figures 4 and 5, the errors in limb-darkening representations cause similar errors. We note, however, that McCullough et al. (2014) fit starspots that changed the transit depth by a few hundred parts per million as opposed to the 100 ppm error we find.

These errors occur at all wavelengths, but are more significant in the near-infrared *H* and *K* bands. The differences in the *H* and *K* bands are up to about 3% of the transit depth due to differences in the curvature of the limb-darkening laws relative to the CLIV. This error may become more important in the era of *Wide Field Infrared Survey Telescope (WFIRST)* and the *James Webb Space Telescope (JWST)*, where we expect to observe infrared transits and measure the wavelength sensitivity of the planetary radius. Because the errors appear to be similar at all wavelengths, we concentrate on the *Kepler* optical band and the infrared *K* band only.

We have computed our planetary transits assuming the small-planet approximation (Mandel & Agol 2002), which some may consider too large. However, we are concerned primarily with the difference between light curves caused by using the limb-darkening law so that errors in our calculation due to the small-planet approximation will cancel. But we stress that this work is a qualitative comparison to investigate

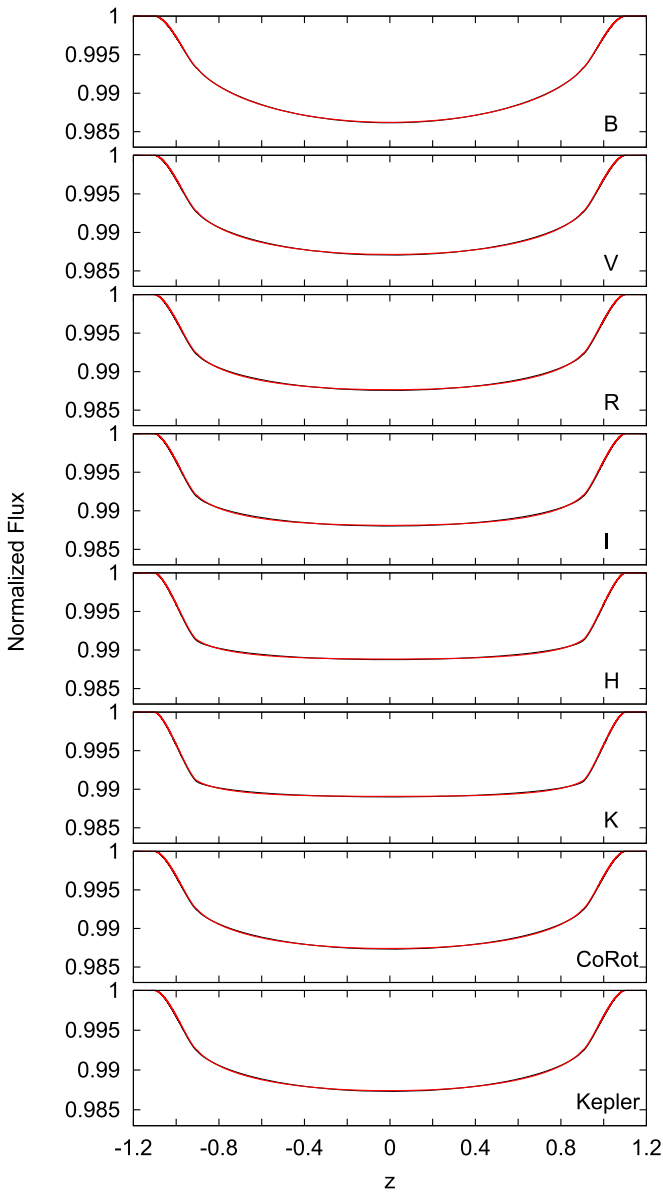


Figure 3. Predicted planetary-transit light curves computed using the small-planet approximation, $R_p/R_* = 0.1$, for a plane-parallel model stellar atmosphere with $T_{\text{eff}} = 5700$ K and $\log g = 4.5$. There is essentially no difference between the transit curves computed using the model CLIV (black) and using the best-fit quadratic limb-darkening law (red).

the role of limb-darkening laws in transit observations. We test this by computing test cases with $R_p/R_* = 0.05$ and 0.01 and plot in Figure 6 the differences between the spherically symmetric model stellar atmosphere CLIV transit light curves and the light curves modeled assuming the quadratic limb-darkening law. To establish a consistent basis of comparison, in this figure we multiply the differences for the $R_p/R_* = 0.05$ and 0.01 cases by 4 and 100, respectively, which are the ratio of surface area blocked by the planet to the star’s surface area compared to the blocked surface for the traditional small-planet approximation, $R_p/R_* = 0.1$.

We see in Figure 6 that between the second and third contact of the transit the planet’s relative size causes almost no change to the differences between the light curves. However, during ingress and egress, the difference as a function of planet size

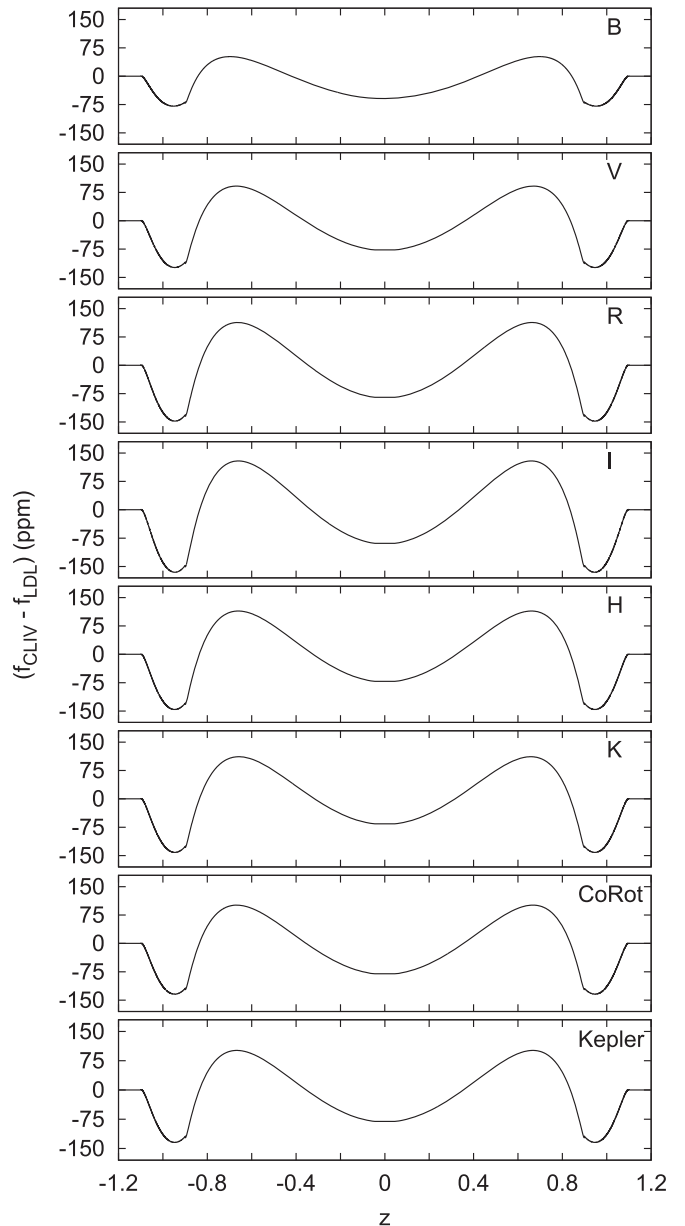


Figure 4. Difference between the transit light curves computed from a plane-parallel model stellar atmosphere CLIV and its best-fit quadratic limb-darkening law from Figure 3 as a function of wavelength.

does not scale with surface area simply because only a fraction of the planet occults the star, suggesting that as the planet size decreases the relative flux difference increases. This means that using the small-planet approximation underestimates the errors at ingress and egress. But the comparison is sufficient to show that our analysis is not significantly affected by assuming the traditional small-planet approximation. The analysis also shows that to first order the error induced by assuming a quadratic limb-darkening law instead of a realistic CLIV scales as a function of the planet’s surface area.

5. Comparison between CLIV and Four-parameter Limb-darkening Laws

Section 4 explored the quadratic limb-darkening law, which is the most commonly used parameterization for modeling

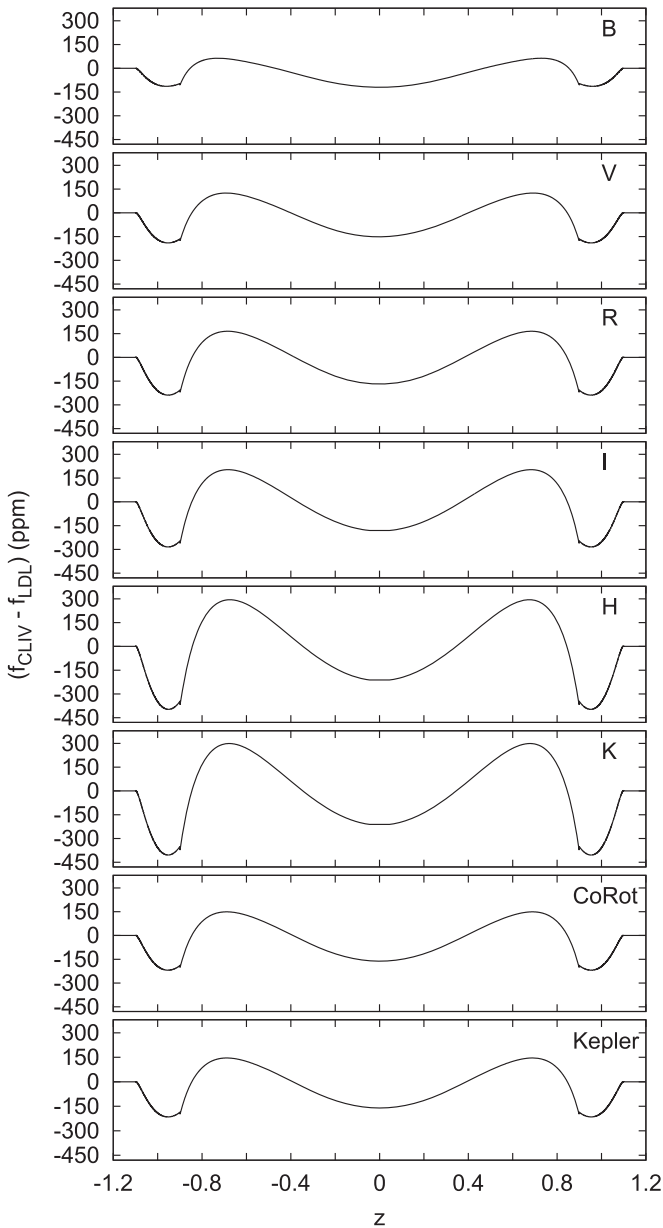


Figure 5. Difference between the transit light curves computed from a spherically symmetric model stellar atmosphere CLIV and its best-fit quadratic limb-darkening law as a function of wavelength.

planetary-transit light curves, but Mandel & Agol (2002) also derived analytic solutions based on the Claret (2000) four-parameter limb-darkening law, which is considered to be a significant improvement relative to other limb-darkening laws. Neilson & Lester (2013a, 2013b) showed that the four-parameter law was the only law out of six commonly assumed parameterizations tested that could reasonably fit CLIV from spherically symmetric model stellar atmospheres. However, this law requires fitting two more free parameters. We note that the three-parameter law of Sing et al. (2009) was not tested, but by its nature the four-parameter limb-darkening law offers a more precise fit to the CLIV, hence we consider that law since it is one of the most precise fits.

We construct synthetic light curves using the best-fit four-parameter limb-darkening law to compare with those computed

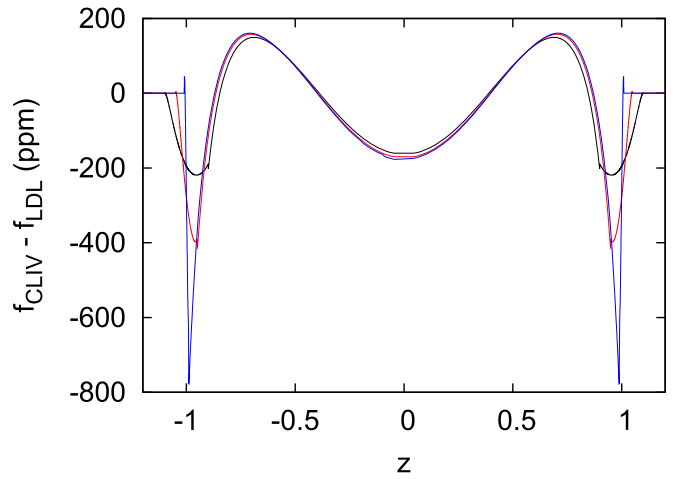


Figure 6. Comparison between the differences between planetary-transit light curves using CLIV and best-fit quadratic limb-darkening laws for three different planet sizes $R_p/R_* = 0.1$ (black), 0.05 (red), and 0.01 (blue) in the *Kepler* waveband. The differences for the smaller planets sizes are scaled by the surface area of the planet relative to the area of the largest planet to allow for a meaningful comparison.

directly from the plane-parallel model stellar atmosphere CLIV and present the *K* band and *Kepler* light curves in Figure 7. There are no noticeable differences between the two light curves at these wavelengths and those presented in previous sections. To explore this more closely, in the right panel of Figure 7 we plot the difference between the light curves in parts per million. It is apparent that the addition of two more free parameters to the limb-darkening law only decrease the difference at ingress/egress by a factor of three, leaving a still significant error for the case of plane-parallel models. The agreement is better at transit center, where the flux difference is about 10 ppm. While not large, it does suggest a small error for measuring planet size.

Next, we repeat the comparison with the more geometrically realistic, spherically symmetric model stellar atmospheres. In Figure 8, we show the synthetic light curves and the flux differences. Again, the planetary-transit light curves are very similar to each other and to the light curves constructed using plane-parallel models. The differences between the spherically symmetric CLIV and the Claret (2000) 4-p limb-darkening law shown in the right panel are ≤ 40 ppm for the *K* band, about a factor of 10 improvement compared with the quadratic limb-darkening law shown in Figure 5. This shows that the 4-p limb-darkening law is a significant improvement on the quadratic limb-darkening law following the fact that the 4-p law is a more accurate fit to spherically symmetric CLIV. This shift in limb-darkening laws will be important as we approach the era of *Transiting Exoplanet Survey Satellite* (*TESS*), *Planetary Transits and Oscillations of Stars* (*PLATO*), and *JWST*, but there will still be some small errors.

It is worth asking how much the relative radius of the planet or the LDC would have to change to minimize the difference between the planetary-transit light curves computed using the CLIV and that computed using the LDCs. One method to test this is to compute a blind Markov Chain Monte Carlo (MCMC) fit of the CLIV light curve that freely fits the LDCs and ρ . However, to perform the MCMC requires injecting noise into the light curve to simulate observational error, which would introduce assumptions about the observations that would make any results dependent on that noise. Instead we are looking at

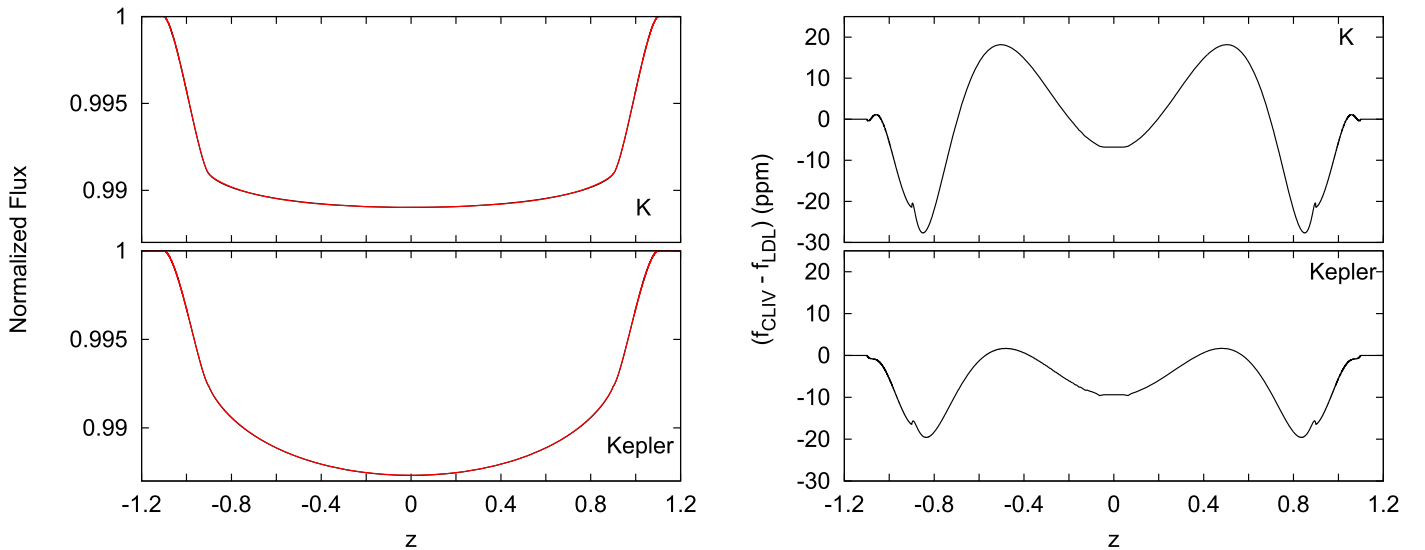


Figure 7. (Left) Synthetic planetary-transit light curves for the *K* band and the *Kepler* band. The CLIVs computed using plane-parallel model stellar atmospheres were used directly and to generate the corresponding four-parameter limb-darkening law. The two light curves are nearly indistinguishable. (Right) The difference between the two light curves from the left panel is in parts per million.

the best-case scenario that probes how the assumption of limb-darkening laws biases results. As such, we consider a different approach.

We vary the relative radius, ρ , until the rms of the flux differences is minimized while holding the coefficients of the limb-darkening law constant. We repeat the analysis varying each coefficient of the limb-darkening law separately and using the same relative radius. To minimize the rms for the *Kepler* band, we find that ρ must be increased by ≈ 240 ppm. Conversely, one could minimize the rms by decreasing the quadratic coefficient of the limb-darkening law, u_2 , by about 0.07 from approximately $u_2 = 0.39$ to $u_2 = 0.32$, but the change in rms is not significant. On the other hand, varying the linear term of the limb-darkening law, u_1 , has little effect on reducing the rms difference. Varying either coefficient changes the predicted stellar flux, and hence the transit depth at any point. However, the shape of the limb-darkening profile is more sensitive to changes of u_1 than to changes of u_2 . Therefore, we see some degeneracy in the *Kepler*-band light curves between the limb darkening and the radius. Repeating the experiment for the *K*-band light curves, we find the changes must be significantly greater to minimize the rms differences. One can either increase ρ by ≈ 450 ppm or decrease u_2 by ≈ 0.2 from 0.75 to 0.55 to resolve the difference.

From this experiment we conclude that if we assume LDCs from model stellar atmospheres that the best-fit planetary radius will have some error simply due to assuming that limb-darkening law. If we allows the LDCs to vary, then we can reduce the remaining error in the radius from ≈ 240 to 180 ppm in the *Kepler* band and to about 200 ppm in the *K* band. This suggests that varying the limb-darkening laws will not correct the error significantly.

6. Significance of the Impact Parameter

In the previous sections, we tested how planetary light curves vary as a function of the geometry of the model stellar atmosphere and the assumed best-fit limb-darkening laws. These calculations have all been for planetary transits across

the center of the stellar disk, that is, for an inclination of 90° or an impact parameter of $b = 0$.

Howarth (2011) and Kipping & Bakos (2011a, 2011b) noted that for many inclined extrasolar planet systems, the limb-darkening laws fit directly to observations differ from predicted limb-darkening laws calculated from model stellar atmospheres. Of course, as noted by Howarth (2011), the inclination of an extrasolar planet’s orbit is probably randomly oriented to our line of sight, making the limb-darkening fit appropriate for a particular inclination different from the limb-darkening fit derived for an equatorial transit. This was especially noted for results presented by Csizmadia et al. (2013) and Lillo-Box et al. (2015).

In this work, we will adopt a different parameter to represent the inclination of the orbit:

$$\mu_0 \equiv \frac{a \cos \theta_0}{R_*} = \frac{a \cos(90^\circ - i)}{R_*}. \quad (11)$$

We choose this definition to connect the inclination with the definition of θ , the angle between a point on the stellar disk and the center of the star. As such, this definition allows us to write the inclination in terms of the variable μ to directly explore the connections between the orbital inclination and the CLIV for modeling transits. For example, if $b = \cos i = 0.5$ for $a/R_* = 1$ and $\mu_0 = \cos(90^\circ - i) = 0.5$, then the CLIV will be probed from the edge of the disk to an angle of $\mu = 0.5$. If the assumed limb-darkening law fits the stellar CLIV accurately, then there would be no problem. However, best-fit limb-darkening coefficients computed from spherically symmetric model stellar atmospheres will be different if we compute them for the whole stellar disk or for only part of it. We show this in Figure 9 for our computed spherically symmetric SATLAS model stellar atmosphere in the *K* and *Kepler* bands.

Figure 9 shows that there is a large dispersion in the limb-darkening coefficients as a function of impact parameter, especially approaching the limb of the star where the CLIV has the largest gradients as a function of μ . The variation is much

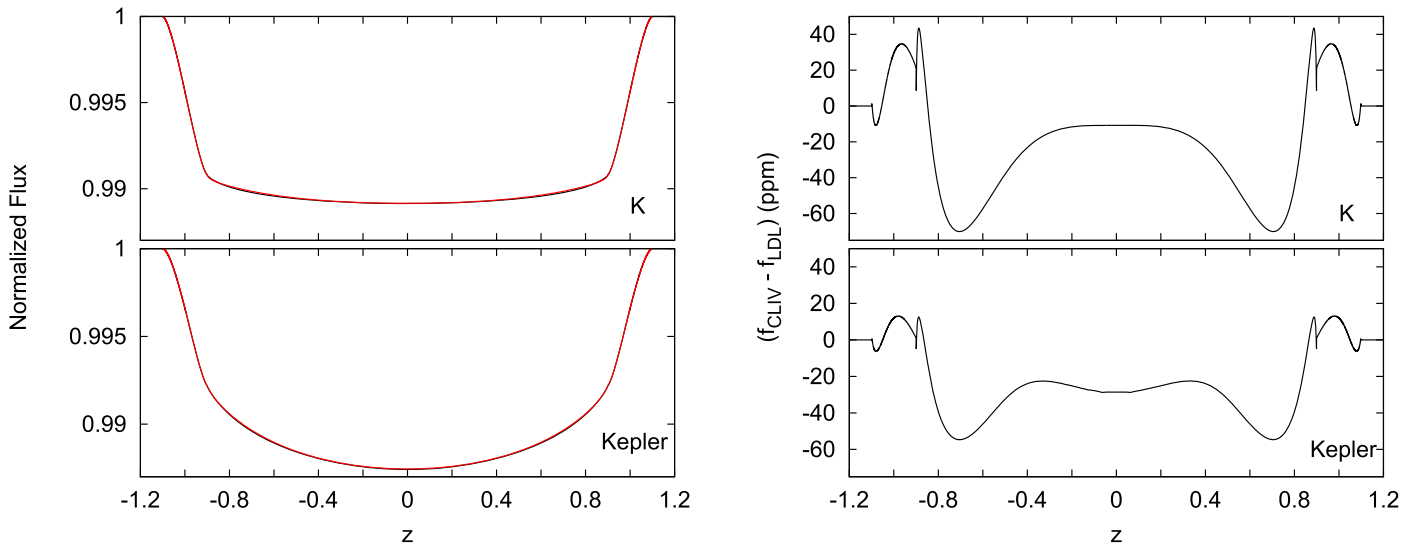


Figure 8. (Left) Synthetic planetary-transit light curves for the *K* band and *Kepler* band. The CLIVs computed using spherically symmetric model stellar atmosphere were used directly and to generate the corresponding four-parameter limb-darkening law. The difference between the two light curves are too small to be seen in the plot. (Right) The difference between the light curves is in parts per million.

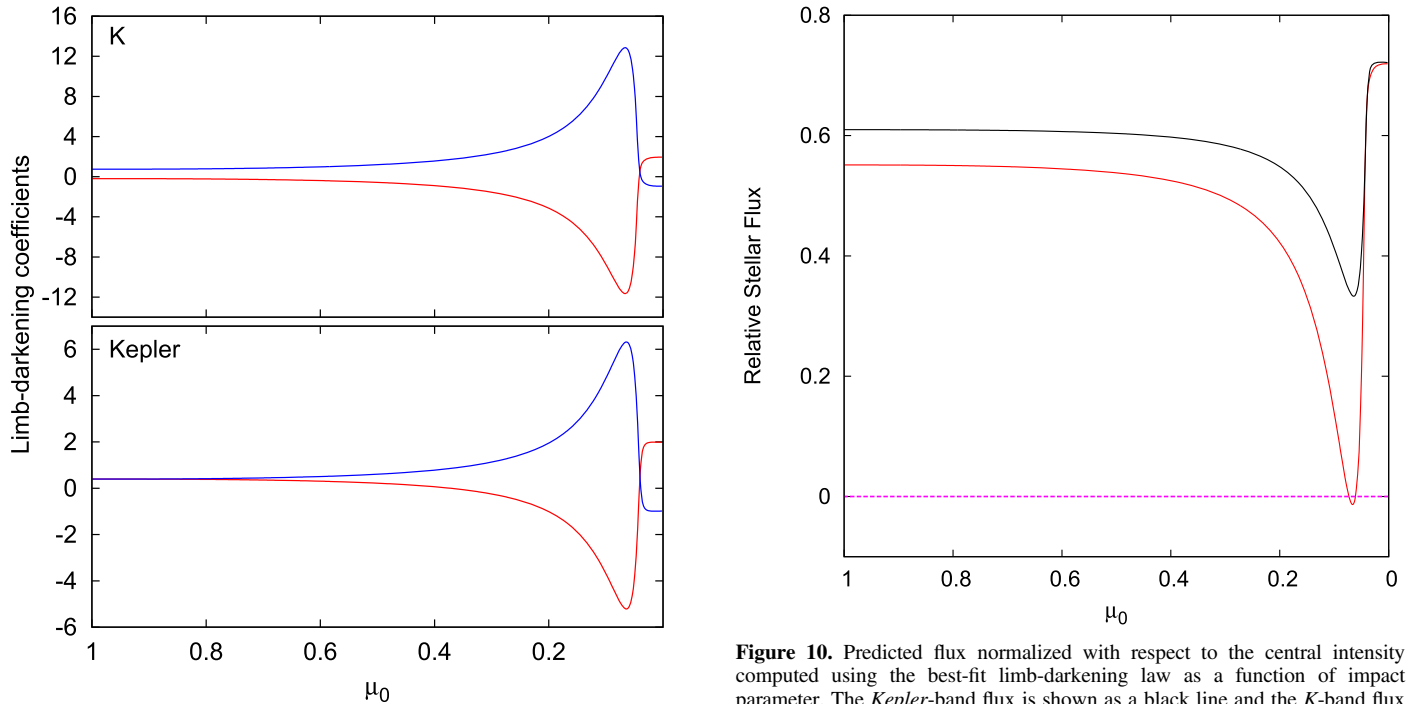


Figure 9. Variation of the best-fit limb-darkening coefficients for the quadratic law (Equation (10)) as a function of impact parameter using the CLIV from the spherically symmetric model stellar atmosphere computed in the previous sections for the *K* band (top) and the *Kepler* band (bottom). The red lines denote the linear coefficient, u_1 , while the blue lines denote the quadratic coefficient, u_2 .

greater than presented in the analysis by Howarth (2011) because we are using more geometrically realistic, spherically symmetric model stellar atmospheres as opposed to plane-parallel models. This suggests that planetary-transit light curves vary significantly as a function of impact parameter and that the impact parameter influences the empirical determination of the limb-darkening parameters. It is notable that for the best-fit coefficients computed here, the predicted stellar flux normalized by the central intensity also varies. The predicted flux from

Figure 10. Predicted flux normalized with respect to the central intensity computed using the best-fit limb-darkening law as a function of impact parameter. The *Kepler*-band flux is shown as a black line and the *K*-band flux as a red line. The dashed magenta line denotes where the flux is zero. Note that the computed negative values are not physical and are caused solely by the computed limb-darkening coefficients.

the best-fit limb-darkening laws is shown in Figure 10. The relative flux becomes slightly negative as $\mu_0 \rightarrow 0$ because the best-fit limb-darkening law cannot accurately map the CLIV of the spherically symmetric atmosphere.

Next, we extend our comparison between model stellar atmosphere CLIV and limb-darkening coefficients to investigate impact parameters, $\mu_0 = 1, 0.8, 0.5$. The limb-darkening coefficients are computed from the entire CLIV as opposed to the approach taken in the hybrid synthetic-photometry/atmospheric-model (SPAM) method of Howarth (2011). Figure 11 shows the differences between light curves computed directly

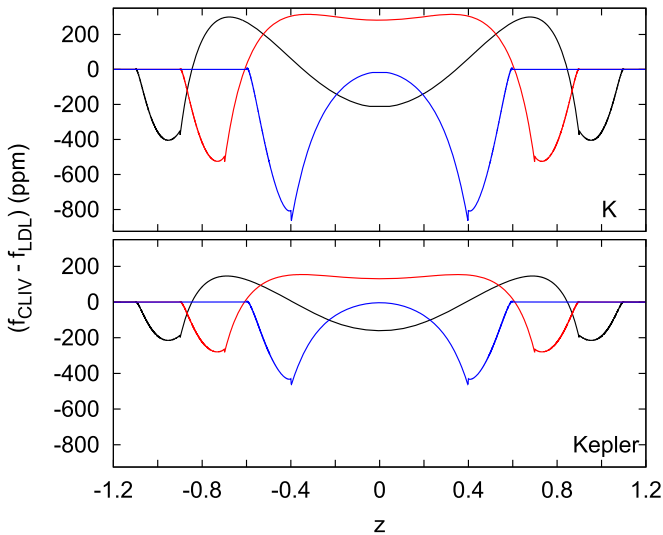


Figure 11. Differences between synthetic light curves computed directly from the spherically symmetric model stellar atmosphere CLIV and the corresponding limb-darkening law for three impact parameters, $\mu_0 = 1$ (black line), 0.8 (red line), and 0.5 (blue line).

from the spherical CLIV and those computed from the limb-darkening law in both the *K* and *Kepler* bands. As $\mu_0 \rightarrow 0$, the errors grow, supporting the need for changing the limb-darkening coefficients as per the SPAM method.

This comparison is generalized in Figure 12 to show the difference between the planetary transits computed directly from the spherical model CLIV and transits computed using limb-darkening laws as a function of impact parameter using the same coefficients for impact parameters (left) and those for the SPAM method (right). The results suggest that the SPAM method can improve the quality of the fits for impact parameters $0.8 \leq \mu_0 \leq 0.6$, but gets much worse for smaller impact parameters.

The results shown in Figure 12 demonstrate the limitations of the SPAM method and why it may improve best fits to planetary-transit observations for only some cases. The results also imply that for observations of systems that are inclined there will be an extra inherent uncertainty because the best-fit limb-darkening coefficients from observations cannot be both a precise fit of the portion of the CLIV and still conserve stellar flux. There is a trade-off.

7. Narrowband Spectral Differences

The analysis presented to this point has concentrated on the differences between broadband spherical model CLIV and best-fit limb-darkening laws. However, it is also important to understand these differences at higher spectral resolution as new observations are exploring spectral properties of extrasolar planets. From our model stellar atmosphere, we compute CLIV at a nominal spectral resolution of 50 and derived the corresponding best-fit limb-darkening coefficients.

The coefficients for the quadratic limb-darkening law are plotted as a function of wavelength in Figure 13 along with those from the broadband coefficients. At the same wavelength, there is close agreement between the broadband coefficients and the coefficients for the higher spectral resolution. However, the higher-resolution coefficients vary significantly at other wavelengths, even including *limb brightening*. At longer wavelengths, the coefficients approach a constant value

because the CLIV is much flatter and more thermal in nature, being influenced by fewer atomic spectral lines. It should be noted that the limb-darkening coefficients do vary slightly due to molecular opacities.

Because of the increasing importance of monochromatic limb darkening and subtle differences with the broadband limb darkening, we compute synthetic planetary-transit models as a function of wavelength assuming an impact parameter $\mu_0 = 1$ using our spherically symmetric model stellar atmosphere. The average difference in flux between the synthetic transits using direct model CLIV and the transits assuming the best-fit limb-darkening coefficients is plotted in Figure 14. The differences are similar to the differences for broadband models.

The difference is greatest in the UV and near-UV where the spectrum contains more lines of ions that vary strongly with depth in the atmosphere. Because the CLIV probes a range of depths, these spectral features prevent a quadratic limb-darkening law from achieving a smooth fit. Of particular interest is that the average difference grows larger, and more negative, going from the optical to the infrared. This may affect finding evidence of important molecules, such as water, from transit spectral observations that can trace the structure of planetary atmospheres. This difference from the *B* to the *K* band is about 180 ppm, implying that past searches that measure flat planet spectra might be contaminated by the assumption of a quadratic limb-darkening law. This is because transit spectroscopy is a relative difference in the planet radius (or surface area) as a function of wavelength. Because the average flux difference in Figure 14 is a measure of the systematic bias of the planetary radius due to the use of this law, it might hide spectral properties of the planet. This would not be an issue for the spectra if the average as a function of wavelength were flat, but we find there is a slope that will contaminate the transit spectra.

These results show that the use of the quadratic limb-darkening law has serious deficiencies, especially toward the infrared wavelengths where the CLIV is more “box”-like. Kreidberg et al. (2014) found that the infrared planetary-transit observations of GJ 1214b could be well modeled using linear limb-darkening laws. However, the linear law is a reasonable representation of the infrared CLIV only over a restricted range from the center of the stellar disk because the intensity decreases dramatically near the limb. This decrease would occur very close to the edge of the disk for a star with the higher gravity of GJ 1214 (Neilson & Lester 2013b) and appears to be consistent with the residuals measured by Kreidberg et al. (2014). We will explore the differences between computing transit light curves assuming CLIV and quadratic limb-darkening laws in a forthcoming article.

These differences as a function of wavelength, which range from about -50 ppm in the *B* band to about -150 ppm in the infrared, could be significant enough to hide features in measured planetary spectra from transit observations. For instance, Brogi et al. (2016) presented measurements of the composition and rotation of HD 189733b using high-resolution infrared spectra, but the spectral features are of the same order of magnitude as the differences presented in Figure 14. Similar issues are apparent in the transit spectra analyzed by Madhusudhan et al. (2014), who also included starspots to fit the observations. This is especially concerning as our results are for low-resolution spectra, while they were using high-resolution spectra for which stellar limb darkening can be more complex.

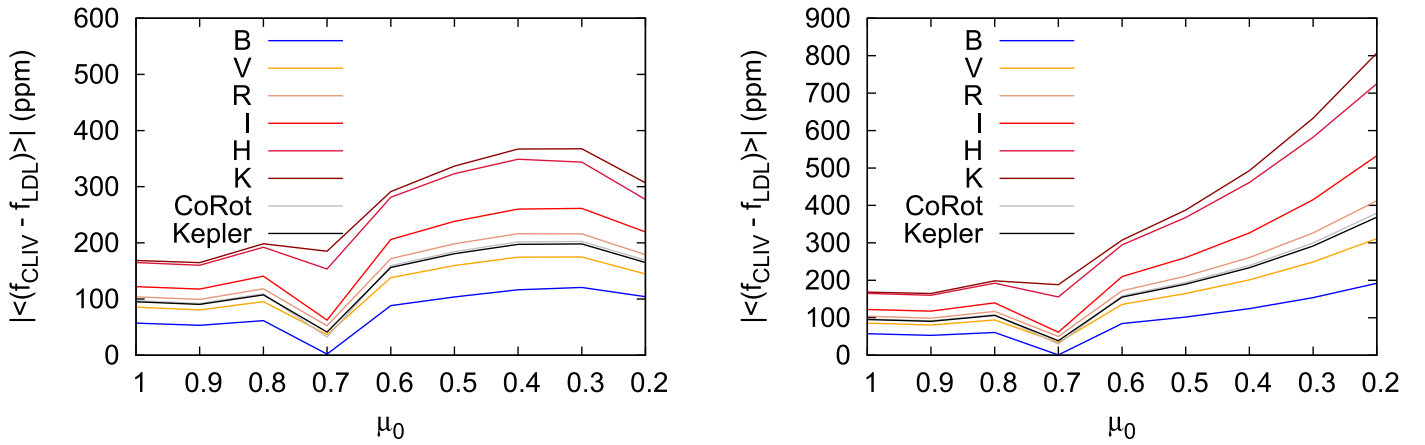


Figure 12. Average difference between planetary-transit light curves computed using model CLIV and limb-darkening laws as a function of impact parameter. Light curves computed using the same limb-darkening coefficients are shown on the left, while those computed using the SPAM method are shown on the right.

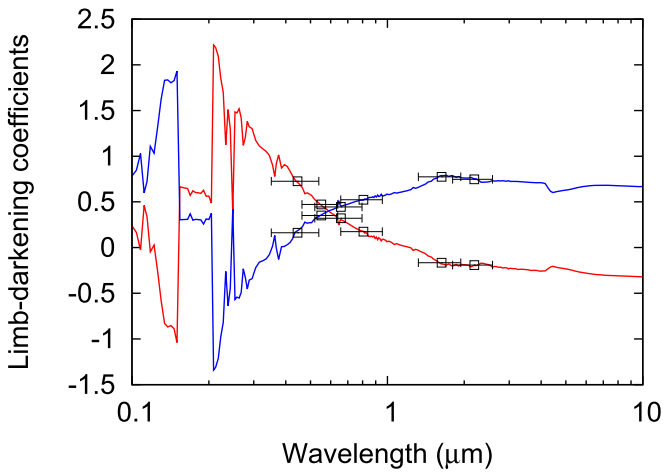


Figure 13. Quadratic limb-darkening coefficients as a function of wavelength with a nominal spectral resolving power of 50. The linear coefficients are shown in red, and the quadratic coefficients are shown in blue. The limb-darkening coefficients for the broadband Johnson filters are plotted as open squares with error bars indicating the bandpass.

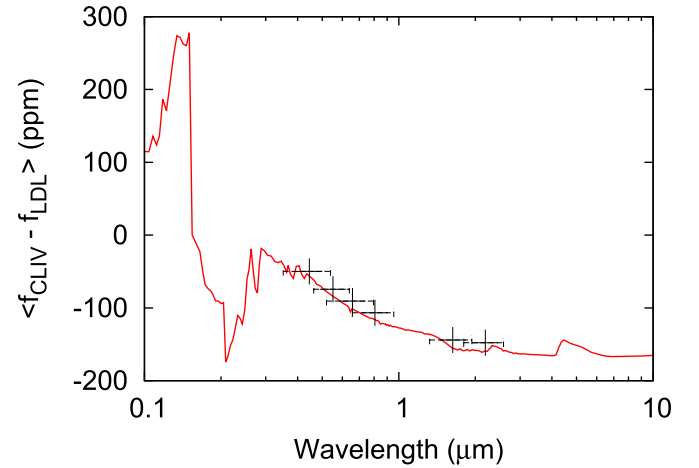


Figure 14. Average differences between synthetic light curves computed directly from spherically symmetric model stellar atmosphere CLIV and their corresponding limb-darkening coefficients as a function of wavelength shown along with the average difference for each Johnson band.

8. Conclusions

In this work, we have demonstrated the importance of stellar CLIV compared to assumed limb-darkening laws for modeling planetary-transit measurements, at least in a qualitative sense. Specifically, we find that synthetic transit light curves computed directly from spherically symmetric model stellar atmosphere CLIV differ significantly from light curves computed assuming traditional quadratic limb-darkening laws. For broadband measurements, these differences are up to about 100–400 ppm at the limb of the star and the average differences range from ~ 50 to ~ 150 ppm. We note that changing from the small-planet approximation to a more realistic method will not significantly change these results. These results also highlight the challenges for measuring high-precision exoplanet properties when assuming simple, parametric limb-darkening laws.

The average difference measured is small but systematic, and it increases toward the infrared, potentially impacting the uncertainty of spectrophotometric transit measurements of extrasolar planet atmospheres. We tested this importance by computing the average difference between light curves computed directly from CLIV and from best-fit limb-darkening laws as a function of wavelength.

We explored the potential of the SPAM method (Howarth 2011) for modeling planetary transits with different impact parameters. While it is certainly essential to take the impact parameter into account, we find a flaw in the SPAM method: by fitting the limb-darkening coefficients to only the part of the star’s CLIV corresponding to the path of the transiting planet, the stellar flux is not measured accurately. As such, the SPAM method is a trade-off: improved modeling of the shape of the limb-darkening profile over the region of interest while decreasing the precision in conserving the stellar flux. One way around this is to use both sets of limb-darkening coefficients: the SPAM coefficients and the coefficients fit to the entire disk to measure the transit.

Our findings suggest that assuming a simple limb-darkening law leads to an intrinsic error for measuring the relative radius of an extrasolar planet and the secondary properties, such as the planet’s atmospheres and oblateness. This error is currently small, ≤ 200 ppm, but as observations push to higher precision and new missions such as *TESS*, *PLATO*, and *JWST* start returning observations, these differences will become more important.

We recommend the following changes to how extrasolar planet transits are modeled:

1. Directly fit the CLIV from spherical model stellar atmospheres to the observations;
2. Switch to the Claret (2000) four-parameter limb-darkening law fit to the CLIV of spherical model stellar atmospheres as a more precise representation of the CLIV; or
3. After fitting observations using a simple quadratic limb-darkening law, compare that law with spherical model stellar atmosphere CLIV (e.g., Neilson & Lester 2013b) to quantify the uncertainty introduced.

In regards to our third recommendation, we will present broadband errors introduced by assuming the quadratic limb-darkening law as a function of stellar properties and orbital inclination in a future paper. However, our first recommendation is our preferred approach. In this case, we shift from fitting limb-darkening coefficients to fitting stellar properties such as effective temperature, gravity, and stellar mass, which offers a way to understand both the planet and its star to a new precision, especially when coupled with other methods such as the flicker–gravity relation (Bastien et al. 2014, 2016).

R.I. is grateful for funding from the NSF (AST-0807664). J.T.M. acknowledges funding from the Honors College at East Tennessee State University. J.B.L. is grateful for support from a Discovery grant from the Natural Sciences and Engineering Research Council of Canada.

ORCID iDs

Hilding R. Neilson  <https://orcid.org/0000-0002-7322-7236>
 Richard Ignace  <https://orcid.org/0000-0002-7204-5502>

References

- Bastien, F. A., Stassun, K. G., Basri, G., & Pepper, J. 2016, *ApJ*, **818**, 43
 Bastien, F. A., Stassun, K. G., & Pepper, J. 2014, *ApJL*, **788**, L9
 Borucki, W. J., Koch, D., Basri, G., et al. 2010, *Sci*, **327**, 977
 Brogi, M., de Kok, R. J., Albrecht, S., et al. 2016, *ApJ*, **817**, 106
 Cabrera, J., Bruntt, H., Ollivier, M., et al. 2010, *A&A*, **522**, A110
 Charbonneau, D., Brown, T. M., Latham, D. W., & Mayor, M. 2000, *ApJL*, **529**, L45
 Chiavassa, A., Collet, R., Casagrande, L., & Asplund, M. 2010, *A&A*, **524**, A93
 Claret, A. 2000, *A&A*, **363**, 1081
 Claret, A. 2009, *A&A*, **506**, 1335
 Claret, A., Hauschildt, P. H., & Witte, S. 2012, *A&A*, **546**, A14
 Csizmadia, S., Pasternacki, T., Dreyer, C., et al. 2013, *A&A*, **549**, A9
 Deming, D., Sada, P. V., Jackson, B., et al. 2011, *ApJ*, **740**, 33
 Dominik, M. 2004, *MNRAS*, **352**, 1315
 Espinoza, N., & Jordán, A. 2015, *MNRAS*, **450**, 1879
 Espinoza, N., & Jordán, A. 2016, *MNRAS*, **457**, 3573
 Fouqué, P., Heyrovský, D., Dong, S., et al. 2010, *A&A*, **518**, A51
 Hellier, C., Anderson, D. R., Cameron, A. C., et al. 2014, *MNRAS*, **440**, 1982
 Howarth, I. D. 2011, *MNRAS*, **418**, 1165
 Kipping, D., & Bakos, G. 2011a, *ApJ*, **730**, 50
 Kipping, D., & Bakos, G. 2011b, *ApJ*, **733**, 36
 Kipping, D. M. 2013, *MNRAS*, **435**, 2152
 Kirk, B., Conroy, K., Prša, A., et al. 2016, *AJ*, **151**, 68
 Knutson, H. A., Charbonneau, D., Noyes, R. W., Brown, T. M., & Gilliland, R. L. 2007, *ApJ*, **655**, 564
 Koch, D. G., Borucki, W. J., Basri, G., et al. 2010, *ApJL*, **713**, L79
 Kreidberg, L., Bean, J. L., Désert, J.-M., et al. 2014, *Natur*, **505**, 69
 Kurucz, R. L. 1979, *ApJS*, **40**, 1
 Kurucz, R. L. 2005, *MSAIS*, **8**, 14
 Lester, J. B., & Neilson, H. R. 2008, *A&A*, **491**, 633
 Lillo-Box, J., Barrado, D., Santos, N. C., et al. 2015, *A&A*, **577**, A105
 Madhusudhan, N., Crouzet, N., McCullough, P. R., Deming, D., & Hedges, C. 2014, *ApJL*, **791**, L9
 Mandel, K., & Agol, E. 2002, *ApJL*, **580**, L171
 McCullough, P. R., Crouzet, N., Deming, D., & Madhusudhan, N. 2014, *ApJ*, **791**, 55
 Mihalas, D. 1978, *Stellar Atmospheres* (2nd ed.; San Francisco, CA: W. H. Freeman and Co.)
 Müller, H. M., Huber, K. F., Czesla, S., Wolter, U., & Schmitt, J. H. M. M. 2013, *A&A*, **560**, A112
 Neilson, H. R., & Lester, J. B. 2011, *A&A*, **530**, A65
 Neilson, H. R., & Lester, J. B. 2012, *A&A*, **544**, A117
 Neilson, H. R., & Lester, J. B. 2013a, *A&A*, **554**, A98
 Neilson, H. R., & Lester, J. B. 2013b, *A&A*, **556**, A86
 Pollacco, D. L., Skillen, I., Collier Cameron, A., et al. 2006, *PASP*, **118**, 1407
 Popper, D. M. 1984, *AJ*, **89**, 132
 Prša, A., & Zwitter, T. 2005, *ApJ*, **628**, 426
 Seager, S., & Hui, L. 2002, *ApJ*, **574**, 1004
 Sing, D. K. 2010, *A&A*, **510**, A21
 Sing, D. K., Désert, J.-M., Lecavelier Des Etangs, A., et al. 2009, *A&A*, **505**, 891
 Wade, R. A., & Rucinski, S. M. 1985, *A&AS*, **60**, 471
 Winn, J. N., Holman, M. J., Bakos, G. Á, et al. 2007, *AJ*, **134**, 1707
 Wittkowski, M., Aufdenberg, J. P., Driebe, T., et al. 2006a, *A&A*, **460**, 855
 Wittkowski, M., Aufdenberg, J. P., & Kervella, P. 2004, *A&A*, **413**, 711
 Wittkowski, M., Hummel, C. A., Aufdenberg, J. P., & Roccatagliata, V. 2006b, *A&A*, **460**, 843
 Zhu, W., Huang, C. X., Zhou, G., & Lin, D. N. C. 2014, *ApJ*, **796**, 67